ADF300322

AD

AD-A133681

TECHNICAL REPORT ARBRL-TR-02521

(Supersedes IMR No. 771)

LIQUID PAYLOAD ROLL MOMENT INDUCED BY A SPINNING AND CONING PROJECTILE

Charles H. Murphy

September 1983

US ARMY ARMAMENT RESEARCH AND DEVELOPMENT COMMAND
BALLISTIC RESEARCH LABORATORY
ABERDEEN PROVING GROUND, MARYLAND

Approved for public release; distribution unlimited.

DTIC FILE COPY

DTIC
ELECTE
OCT 04 1983
S D
E

88 10 05 050

Destroy this report when it is no longer needed.
Do not return it to the originator.

Additional copies of this report may be obtained from the National Technical Information Service, U. S. Department of Commerce, Springfield, Virginia 22161.

The findings in this report are not to be construed as an official Department of the Army position, unless so designated by other authorized documents.

The use of trade names or manufacturers' names in this report does not constitute indorsement of any commercial product.

UNCLASSIFIED

SECURITY CLASSIFICATION OF THIS PAGE (When Data Entered)

REPORT DOCUMENTATION PAGE		READ INSTRUCTIONS BEFORE COMPLETING FORM
1. REPORT NUMBER TECHNICAL REPORT ARBRL-TR-02521	2. GOVT ACCESSION NO. AD-A133 681	3. RECIPIENT'S CATALOG NUMBER
4. TITLE (and Subtitle) LIQUID PAYLOAD ROLL MOMENT INDUCED BY A SPINNING AND CONING PROJECTILE		5. TYPE OF REPORT & PERIOD COVERED Final 6. PERFORMING ORG. REPORT NUMBER
7. AUTHOR(s) Charles H. Murphy		8. CONTRACT OR GRANT NUMBER(s)
9. PERFORMING ORGANIZATION NAME AND ADDRESS US Army Ballistic Research Laboratory ATTN: DRDAR-BLL Aberdeen Proving Ground, Maryland 21005		10. PROGRAM ELEMENT PROJECT, TASK AREA & WORK UNIT NUMBERS RDT&E 1L161102AH43
11. CONTROLLING OFFICE NAME AND ADDRESS US Army Armament Research & Development Command US Army Ballistic Research Laboratory (DRDAR-BLA-S) Aberdeen Proving Ground, Maryland 21005		12. REPORT DATE September 1983 13. NUMBER OF PAGES 53
14. MONITORING AGENCY NAME & ADDRESS(if different from Controlling Office)		15. SECURITY CLASS. (of this report) Unclassified 15a. DECLASSIFICATION/DOWNGRADING SCHEDULE

16. DISTRIBUTION STATEMENT (of this Report)

Approved for public release, distribution unlimited.

17. DISTRIBUTION STATEMENT (of the abstract entered in Block 20, if different from Report)

18. SUPPLEMENTARY NOTES

This report supersedes IMR-771, dated March 1983.

19. KEY WORDS (Continue on reverse side if necessary and identify by block number)

Liquid Payload
Liquid Roll Moment
Liquid Side Moment
Liquid-Filled Projectile
Spinning Projectile

20. ABSTRACT (Continue on reverse side if necessary and identify by block number) (bja)

The linear theory for a coning and spinning liquid payload has been extended to the calculation of a quadratic roll moment. The resulting quadratic roll moment coefficient is shown to be exactly the negative of the linear side moment coefficient for constant amplitude coning motion. This relationship between side moment and roll moment has been observed for projectiles with moving solid components and has encouraging experimental support for liquid payloads.

DD FORM 1 JAN 73 1473 EDITION OF 1 NOV 65 IS OBSOLETE

UNCLASSIFIED

SECURITY CLASSIFICATION OF THIS PAGE (When Data Entered)

TABLE OF CONTENTS

		Page
	LIST OF FIGURES	5
I.	INTRODUCTION	7
II.	LIQUID ROLL MOMENT	9
III.	LIQUID ROLL MOMENT THEORY	12
	Table 1. Experimental Values of C_{LRM}	13
IV.	DISCUSSION	18
V.	SUMMARY	19
	REFERENCES	26
	APPENDIX A	29
	APPENDIX B	33
	APPENDIX C	39
	LIST OF SYMBOLS	43
	DISTRIBUTION LIST	47

Accession For
NTIS GRA&I ☒
DTIC TAB ☐
Unannounced ☐
Justification
By
Distribution/
Availability Codes
Dist | Avail and/or Special
A

PREVIOUS PAGE IS BLANK

LIST OF FIGURES

Figure		Page
1	C_{LRM} From Gyroscope Tests (Ref. 15), c/a = 4.291	20
2	C_{LSM} vs τ for Re = 10^6, ε = 0, and the D'Amico-Miller Parameters: c/a = 4.291, f = 1	21
3	C_{LSM} vs τ for Re = 10^5, ε = 0, and the D'Amico-Miller Parameters: c/a = 4.291, f = 1	22
4	C_{LSM} vs τ for Re = 10^4, ε = 0, and the D'Amico-Miller Parameters: c/a = 4.291, f = 1	23
5	C_{LSM} vs τ for Re = 10^3, ε = 0, and the D'Amico-Miller Parameters: c/a = 4.291, f = 1	24
6	C_{LSM} vs τ for Re = 10^2, ε = 0, and the D'Amico-Miller Parameters: c/a = 4.291, f = 1	25

PREVIOUS PAGE IS BLANK

I. INTRODUCTION

In 1958 Karpov and Bradley[1] observed short flights of shell, accompanied by substantial reductions in spin rates. An eleven percent range reduction, for example, was accompanied by a fifty percent reduction in spin over thirty seconds. Later tests showed that the spin loss occurs after the coning motion exceeds ten degrees and is not the cause of growth in the coning motion. It was shown[2-3] in 1977 that this coning growth and spin decay could be explained by the motion of loose internal components. It should be emphasized that in all monitored flights of projectiles with large coning motion and no loose internal parts, no large despin moments have been observed. Thus, the combined presence of a large coning motion and a large despin moment is symptomatic of a loose internal component.

In the summer of 1974, a 155mm shell with a liquid payload was fired with a yawsonde telemetry unit[4] and this projectile developed a coning motion with amplitude in excess of forty degrees.[5] When the coning motion exceeded forty degrees, the telemetry record showed a very rapid despin of forty percent in less than five seconds. Since 1974, six more observations of liquid-filled 155mm projectiles with large coning motions and large despin rates have been made.[6-8] In addition, thirty-six observations have been made of large coning

---

1. *B.G. Karpov and J.W. Bradley, "A Study of Causes of Short Ranges of the 8" T317 Shell," BRL Report 1049, May 1958 (AD 377548).*

2. *C.H. Murphy, "Influence of Moving Internal Parts on Angular Motion of Spinning Projectiles," Journal of Guidance and Control, Vol. 1, March-April 1978, pp. 117-122. See also BRL-MR-2731, February 1977 (AD A037338).*

3. *W.G. Soper, "Projectile Instability Produced by Internal Friction," AIAA Journal, Vol. 16, Jan 1978, pp. 8-11.*

4. *W.H. Mermagen, "Measurements of the Dynamical Behavior of Projectiles Over Long Flight Paths," Journal of Spacecraft and Rockets, Vol. 8, April 1971, pp. 380-385. See also BRL MR-2079, November 1970 (AD 717002).*

5. *W.P. D'Amico, V. Oskay, W.H. Clay, "Flight Tests of the 155mm XM687 Binary Projectile and Associated Design Modification Prior to the Nicolet Winter Test 1974-1975," BRL-MR-2748, May 1977 (AD B019969).*

6. *W.P. D'Amico, W.H. Clay, and A. Mark, "Yawsonde Data for M687-Type Projectiles with Application to Rapid Spin Decay and Stewartson-Type Spin-Up Instabilities," ARBRL-MR-03027, June 1980 (AD A089646).*

7. *W.P. D'Amico, W.H. Clay, and A. Mark, "Diagnostic Tests for Wick-Type Payloads and High-Viscosity Liquids," ARBRL-MR-02913, April 1979 (AD A072812).*

8. *W.P. D'Amico and W. H. Clay, "High Viscosity Liquid Payload Yawsonde Data for Small Launch Yaws," ARBRL-MR-03029, June 1980 (AD A088411).*

PREVIOUS PAGE IS BLANK

motions and despin moments for projectiles with payloads of liquid-solid mixtures; namely, twenty-six XM61 projectiles containing liquid plus cotton wicks[7,9-11] and ten XM825 projectiles containing liquid plus felt wedges.[12-14] Indeed, all observed flights of projectiles with liquid or liquid-solid payloads that performed large coning motion exhibited large losses in spin.

This characteristic association of a large despin moment with a large coning motion for a projectile with a moving payload can become a diagnostic tool. Miller[15] suggested using this tool to determine the existence of small amplitude unstable liquid-induced side moments. Spin measurements made during coning motion on a gyroscope predicted flight pitch instabilities caused by very viscous liquids, and these were observed in flight.[16] The original M687 flight instability was caused by a large external Magnus moment, even though the liquid caused a rapid despin. Thus the assumed connection between large coning motion roll moments and small coning motion side moments may have been fortuitous for the case of very viscous payloads.

The linear liquid-induced side moment was first computed by Stewartson[17] for an inviscid liquid payload by use of eigenfrequencies determined by the

---

9. *W.P. D'Amico, "Early Flight Experiences With the XM761," BRL-MR-2791, September 1977 (AD B024975L).*

10. *W.P. D'Amico, "Field Tests of the XM761: First Diagnostic Test," BRL-MR-2792, September 1977 (AD B024976L).*

11. *W.P. D'Amico, "Field Tests of the XM761: Second Diagnostic Test," ARBRL-MR-02806, January 1978 (AD B025305L).*

12. *W.P. D'Amico, "Aeroballistic Testing of the XM825 Projectile: Phase I," ARBRL-MR-02911, March 1979 (AD B037680).*

13. *W.P. D'Amico, "Aeroballistic Testing of the XM825 Projectile: Phase II," ARBRL-MR-03072, January 1981 (AD A098036).*

14. *W.P. D'Amico, "Aeroballistic Testing of the XM825 Projectile: Phase III, High Muzzle Velocity and High Quadrant Elevation," ARBRL-MR-03196, September 1982 (AD B068511L).*

15. *M.C. Miller, "Flight Instabilities of Spinning Projectiles Having Non-rigid Payloads," Journal of Guidance, Control, and Dynamics, Vol. 5, March-April 1982, pp. 151-157.*

16. *W.P. D'Amico and M.C. Miller, "Flight Instability Produced by a Rapidly Spinning, Highly Viscous Liquid," Journal of Spacecraft and Rockets, Vol. 16, Jan-Feb 1979, pp. 62-64.*

17. *K. Stewartson, "On the Stability of a Spinning Top Containing Liquid," Journal of Fluid Mechanics, Vol. 5, Part 4, September 1959, pp. 577-592.*

fineness ratio of the cylindrical container. Wedemeyer[18] introduced boundary layers on the walls of the container and was able to determine viscous corrections for Stewartson's eigenfrequencies, which could then be used in Stewartson's side moment calculation. Murphy[19] then completed the linear boundary layer theory by including all pressure and wall shear contributions to the liquid-induced side moment. The Stewartson-Wedemeyer eigenvalue calculations have been improved at low Reynolds number by Kitchens et al[20] through the replacement of the cylindrical wall boundary approximation by a linearized Navier-Stokes approach. Next, Gerber et al[21-22] extended this linearized NS technique to compute better side moment coefficients for Reynolds numbers less than 10,000.

The only theoretical work on liquid-induced roll moments was done by Vaughn[23] in 1978. Although fair agreement with Miller's data was obtained, the work was marred by some hard-to-justify algebraic steps. It is the purpose of this report to compute the roll moment associated with the linear perturbation flow of Reference 19.

II. LIQUID ROLL MOMENT

The pitching and yawing motion of a symmetric spinning projectile can be represented as the sum of two rotating exponentially growing two-dimensional vectors. In terms of complex variables, this relationship assumes the form[24]

---

18. *E.H. Wedemeyer, "Viscous Correction to Stewartson's Stability Criterion," BRL-R-1325, June 1966 (AD 489687).*

19. *C.H. Murphy, "Angular Motion of a Spinning Projectile with a Viscous Liquid Payload," Memorandum Report ARBRL-MR-03194, August 1982 (AD A118676). See also Journal of Guidance, Control, and Dynamics, Vol. 6, July-August 1983, pp. 280-286.*

20. *C.W. Kitchens, Jr., N. Gerber, and R. Sedney, "Oscillations of a Liquid in a Rotating Cylinder: Solid Body Rotation," BRL Technical Report ARBRL-TR-02081, June 1978 (AD A057759).*

21. *N. Gerber, R. Sedney, and J.M. Bartos, "Pressure Moment on a Liquid-Filled Projectile: Solid Body Rotation," BRL Technical Report ARBRL-TR-02422, October 1982 (AD A120567).*

22. *N. Gerber and R. Sedney, "Moment on a Liquid-Filled Spinning and Nutating Projectile: Solid Body Rotation," BRL Technical Report ARBRL-TR-02470, February 1983 (AD A125332).*

23. *H.R. Vaughn, "Flight Dynamic Instabilities of Fluid-Filled Projectiles," Sandia Laboratories, Albuquerque, NM, SAND 78-0999, June 1978.*

24. *C.H. Murphy, "Free Flight Motion of Symmetric Missiles," BRL-R-1216, July 1963 (AD 442757).*

$$\tilde{\xi} \equiv \tilde{\beta} + i\,\tilde{\alpha} = K_1 e^{i\phi_1} + K_2 e^{i\phi_2} \tag{2.1}$$

where $\ln (K_j/K_{j0}) = \epsilon_j\ \tau_j |\dot{\phi}| t$

$\phi_j = \phi_{j0} + \tau_j \dot{\phi} t$ and

$\dot{\phi}$ is the roll rate.

The transverse moment exerted by a liquid payload was expressed in Reference 19* in the following form.

$$M_{LY} + i\,M_{LZ} = m_L\ a^2 \dot{\phi}^2\ [\tau_1\ C_{LM_1}\ K_1 e^{i\phi_1} + \tau_2\ C_{LM_2}\ K_2 e^{i\phi_2}] \tag{2.2}$$

where

m_L = mass of liquid in fully filled container

and

a = maximum radius of liquid container.

For linear fluid motion, C_{LM_1} should depend on τ_1, ϵ_1, time, Reynolds number, fill ratio, shape of cavity, and direction of spin. A similar remark applies to C_{LM_2}.

The C_{LM_j} are complex quantities whose imaginary parts represent in-plane moments causing rotation in the plane of exp $(i\phi_j)$ and whose real parts represent side moments causing rotation out of the plane of exp $(i\phi_j)$. Thus, C_{LM_j} with its dependence on the direction of spin can be written as

$$C_{LM_j} = \gamma\ C_{LSM_j} + i\ C_{LIM_j} \tag{2.3}$$

where C_{LSM_j}, C_{LIM_j} are real and $\gamma = \dot{\phi}/|\dot{\phi}|$.

Since relations from Reference 19 are used throughout this report, an errata for Reference 19 is given in Appendix A.

The liquid roll moment can now be defined in a similar way. Symmetry considerations imply an even dependence on coning amplitudes and an odd dependence on spin rate.

$$\therefore M_{LX} = m_L a^2 \dot{\phi}|\dot{\phi}| [C_{LRM_0} + \tau_1 K_1^2 C_{LRM_1} + \tau_2 K_2^2 C_{LRM_2}] \tag{2.4}$$

where C_{LRM_j} are functions of Reynolds number, fill ratio, shape of cavity, and time. In addition, for j = 1 and 2, the C_{LRM_j} may be functions of τ_j, ε_j and K_j^2. C_{LRM_0} is the roll moment coefficient exerted by the liquid during spin-up and is zero when steady state is reached. For the steady-state coning motion considered in the Stewartson-Wedemeyer theory ($K_2 = 0$), only one roll moment coefficient is present and we will omit the subscript on τ_1 and C_{LRM_1}:

$$M_{LX} = m_L a^2 \dot{\phi}|\dot{\phi}| \tau K_1^2 C_{LRM}. \tag{2.5}$$

Throughout this report, we will consider only roll moments that can be approximated by the one-term Eq. (2.5) rather than the more complete three-term Eq. (2.4) and will consider only positive spin, $\dot{\phi}$.

The roll rate of a projectile in flight is controlled by the sum of the internal liquid roll moment and the external aerodynamic roll damping moment. For pure coning motion

$$I_x \ddot{\phi} = \left(\frac{\rho V^2}{2}\right) S\ell \left(\frac{\dot{\phi}\ell}{V}\right) C_{\ell_p} + m_L a^2 \dot{\phi}^2 \tau K_1^2 C_{LRM} \tag{2.6}$$

For the liquid payloads, the large increase in roll moment usually occurs suddenly when the coning motion amplitude exceeds 30°. On the other hand, the liquid/solid XM761/XM825 payloads produce large roll moments at a much lower coning amplitude of 10-15°. For all payloads, the coning motion increases rapidly to a steady-state amplitude of 40-45°.

Since definitions (2.1, 2.2, 2.4) were for small coning angles, more precise expressions are required for angles in excess of ten degrees. The yaw plane is the plane containing the missile axis and the velocity vector. The angle between the two vectors is the total angle of attack, α_t. The amplitude of the complex variable $\tilde{\xi}$ is $\sin \alpha_t$ and the argument of $\tilde{\xi}$ is the phase angle of the yaw plane about the missile axis. For the pure coning motion of Eq. (2.5), the exact definition of K_1 is

$$K_1 = |\tilde{\xi}| = \sin \alpha_t \tag{2.7}$$

Unfortunately, the yawsonde data for the XM761/XM825 flights were too poor to yield numerical values of the liquid roll moment coefficient. Seven flights of the M687 payloads did have sufficiently good data and their liquid roll moment values could be computed from Eq. (2.6). The change in roll acceleration at high cone angles, $\Delta \ddot{\phi}$, can be easily obtained from the yawsonde data. From Eq. (2.6)

$$\Delta \ddot{\phi} = (m_L \, a^2/I_x) \, \dot{\phi}^2 \tau \, K_1^2 \, C_{LRM} \tag{2.8}$$

Table 1 gives the seven M687 values of the roll moment coefficient. For very low Reynolds number, a value of about -.04 seems representative while a high Reynolds number value of -.01 is indicated. Since Round 7254 was not completely filled, it is an isolated value. Miller's gyroscope data[15] is given in Figure 1 and indicates a range of -.001 to -.05 for C_{LRM}. Two recently obtained values of roll moment for eight-inch shell[25] are also given in Table 1. Since the flight data were poorly resolved during spin-down, the liquid roll moment coefficients of Table 1 should be considered estimates with accuracies no better than 30%.

III. LIQUID ROLL MOMENT THEORY

Two coordinate systems will be used in this report: the nonrolling aeroballistic XYZ system whose $\hat{X}$-axis is fixed along the missile's axis of symmetry and the inertial XYZ system whose X-axis is tangent to the trajectory at time zero.* Both coordinate systems have origins at the center of the cylindrical payload cavity, which is assumed to be at the center of mass of the projectile. Location in the cavity can be specified in the aeroballistic system by the cylindrical coordinates $\hat{x}$, $\hat{r}$, $\hat{\theta}$ and in the inertial system by x, r, θ. The boundary of the cavity is given by $\hat{x} = \pm c$ and $\hat{r} = a$ where 2c is the height of the cavity. Linear relations between cylindrical coordinates in the two coordinate systems were derived in Reference 19:

$$\hat{x} = x - r \, K_1 \cos(\phi_1 - \theta) \tag{3.1}$$

$$\hat{r} = r + x \, K_1 \cos(\phi_1 - \theta) \tag{3.2}$$

---

* *The trajectory can be well approximated by a straight line for a number of periods of the angular motion.*

25. *W. P. D'Amico and R. J. Yalamanchili, "Yawsonde Tests of the 8-Inch XM877 Binary Projectile: Phase I," BRL Memorandum Report in preparation.*

TABLE 1. EXPERIMENTAL VALUES OF C_{LRM}

Rd No	Re	c/a	$m_L a^2 / I_x$	$\dot{\phi}$ (rad/s)	α_t (deg)	τ	C_{LRM}	Ref
7254*	8.6×10^5	4.39	.0768	500	45	.09	-.040*	5
9357	1.8×10^6	4.97	.0859	500	45	.09	-.020	6
9391	10	4.33	.1615	500	40	.11	-.070	7
9394	10	4.33	.1615	500	40	.11	-.052	7
9540	10	4.33	.1615	470	45	.12	-.045	8
9542	10	4.33	.1615	470	45	.12	-.035	8
9543	10	4.33	.1615	470	45	.12	-.045	8
11-8**	45.2	4.23	.067	942	37.5	.127	-.057	25
12-8**	45.2	4.23	.067	942	40.0	.127	-.060	25
Gyroscope	10^{-1}-10^6	4.29	.488	315	20	.19	See Fig 1	15

* Fill ratio was .87 for Round 7254; all other rounds were 100% fill.

** 8-inch XM877 projectiles.

$$\tilde{\theta} = \theta + (x/r)\, K_1 \sin(\phi_1 - \theta) \tag{3.3}$$

Since the gradient vector for the surface $\tilde{x} = f(x, r, \theta)$ is a vector in the direction of increasing $\tilde{x}$, the unit vector in the direction of increasing $\tilde{x}$ is

$$\vec{e}_{\tilde{x}} = \left(\frac{\partial f}{\partial x}, \frac{\partial f}{\partial r}, \frac{\partial f}{r\partial\theta}\right)\left[\left(\frac{\partial f}{\partial x}\right)^2 + \left(\frac{\partial f}{\partial r}\right)^2 + \left(\frac{\partial f}{r\partial\theta}\right)^2\right]^{-1/2} = (e_{\tilde{x}x}, e_{\tilde{x}r}, e_{\tilde{x}\theta}) \tag{3.4}$$

In a similar way, unit vectors in the direction of increasing $\tilde{r}$ and $\tilde{\theta}$ can be computed in inertia system cylindrical coordinates. These unit vectors along the aeroballistic cylindrical axes are:

$$\begin{aligned}\vec{e}_{\tilde{x}} &= (e_{\tilde{x}x}, e_{\tilde{x}r}, e_{\tilde{x}\theta}) \\ &= \Big(1, -K_1 \cos(\phi_1 - \theta), -K_1 \sin(\phi_1 - \theta)\Big)\end{aligned} \tag{3.5}$$

$$\begin{aligned}\vec{e}_{\tilde{r}} &= (e_{\tilde{r}x}, e_{\tilde{r}r}, e_{\tilde{r}\theta}) \\ &= \Big(K_1 \cos(\phi_1 - \theta), 1, K_1 (x/r) \sin(\phi_1 - \theta)\Big)\end{aligned} \tag{3.6}$$

$$\begin{aligned}\vec{e}_{\tilde{\theta}} &= (e_{\tilde{\theta}x}, e_{\tilde{\theta}r}, e_{\tilde{\theta}\theta}) \\ &= \Big(K_1 \sin(\phi_1 - \theta), -K_1 (x/r) \sin(\phi_1 - \theta), 1\Big)\end{aligned} \tag{3.7}$$

Eqs. (3.5 - 3.7) are correct to terms of order K_1^2.

Since compressive viscous shear is neglected in boundary layer flows, the components of the shear tensor in cylindrical coordinates have the very simple form[26]

$$\tau_{xx} = \tau_{rr} = \tau_{\theta\theta} = -p \tag{3.8}$$

$$\tau_{xr} = \tau_{rx} = \mu\left[\frac{\partial V_r}{\partial x} + \frac{\partial V_x}{\partial r}\right] \tag{3.9}$$

---

26. *H. Schlichting, "Boundary Layer Flow," McGraw-Hill Book Company, New York, 1960, p. 54.*

$$\tau_{x\theta} = \tau_{\theta x} = \mu \left[\frac{\partial V_\theta}{\partial x} + \frac{1}{r} \frac{\partial V_x}{\partial \theta} \right] \tag{3.10}$$

$$\tau_{r\theta} = \tau_{\theta r} = \mu \left[r \frac{\partial (V_\theta / r)}{\partial r} + \frac{1}{r} \frac{\partial V_r}{\partial \theta} \right] \tag{3.11}$$

The stress vector on an area element of the <u>interior</u> lateral cylindrical surface of the liquid container is

$$d\vec{F}_\ell = (dF_{\ell x}, dF_{\ell r}, dF_{\ell \theta}) \tag{3.12}$$

where

$$dF_{\ell x} = - \left[e_{\tilde{r}x} \tau_{xx} + e_{\tilde{r}r} \tau_{rx} + e_{\tilde{r}\theta} \tau_{\partial x} \right]_{\tilde{r}=a} a \, d\tilde{x} \, d\tilde{\theta}$$

$$dF_{\ell r} = - \left[e_{\tilde{r}x} \tau_{xr} + e_{\tilde{r}r} \tau_{rr} + e_{\tilde{r}\theta} \tau_{\theta r} \right]_{\tilde{r}=a} a \, d\tilde{x} \, d\tilde{\theta}$$

$$dF_{\ell \theta} = - \left[e_{\tilde{r}x} \tau_{x\theta} + e_{\tilde{r}r} \tau_{r\theta} + e_{\tilde{r}\theta} \tau_{\theta\theta} \right]_{\tilde{r}=a} a \, d\tilde{x} \, d\tilde{\theta}$$

The corresponding roll moment differential is

$$dM_{\tilde{x}\ell} = a \, \vec{e}_{\tilde{\theta}} \cdot d\vec{F}_\ell$$

$$\doteq - \left\{ \tau_{r\theta} + [\tau_{xr} \sin(\phi_1 - \theta) + \tau_{x\theta} \cos(\phi_1 - \theta)] K_1 \right\}_{\tilde{r}=a} a^2 \, d\tilde{x} \, d\tilde{\theta} \tag{3.13}$$

For the boundary layer on the lateral wall, only derivatives normal to the wall need be considered.

$$\tau_{xr} = \mu \frac{\partial V_x}{\partial r} \tag{3.14}$$

$$\tau_{x\theta} = 0 \tag{3.15}$$

$$\tau_{r\theta} = \mu\, r \frac{\partial(V_\theta/r)}{\partial r} \tag{3.16}$$

The roll moment differential on the forward and rear end walls (j = 1, 2) can be computed in a similar manner.

$$dM_{\hat{x}ej} = \mp \Big\{ \tau_{x\theta} - [\tau_{xr}\,(x/r)\,\sin\,(\phi_1-\theta) \tag{3.17}$$

$$+ \tau_{r\theta}\cos\,(\phi_1-\theta)]\;\hat{K}_1 \Big\}_{\hat{x}=\pm c} \quad \hat{r}^2\, d\hat{r}\, d\hat{\theta}$$

On the endwall only derivatives with respect to x are important.

$$\tau_{xr} = \mu \frac{\partial V_r}{\partial x} \tag{3.18}$$

$$\tau_{x\theta} = \mu \frac{\partial V_\theta}{\partial x} \tag{3.19}$$

$$\tau_{r\theta} = 0 \tag{3.20}$$

We will now compute the quadratic liquid roll moment under the restrictive assumption that only linear fluid mechanics terms need be considered. In Reference 19, the velocity components were expanded in terms of perturbation velocities that were linear in $\hat{K}$.

$$V_x = R\left\{u_s\, e^{s\phi - i\theta}\right\}(a\dot{\phi}) \tag{3.21}$$

$$V_r = R\left\{v_s\, e^{s\phi - i\theta}\right\}(a\dot{\phi}) \tag{3.22}$$

$$V_\theta = r\dot{\phi} + R\left\{w_s\, e^{s\phi - i\theta}\right\}(a\dot{\phi}) \tag{3.23}$$

where

$$s = (\varepsilon + i)\,\tau$$

and where u_s, v_s, w_s are functions of r and x and are linear in $\hat{K}$. Eqs. (3.21-3.23) give the velocity components in terms of x, r, θ. In computing the linear liquid side and in-plane moments, x, r, θ could simply be replaced by $\hat{x}$, $\hat{r}$, $\hat{\theta}$. The liquid roll moment, however, is a quadratic function of K_1 and Eqs. (3.1-3.3) must be used. A useful approximation for this change of variables is

$$h\,(r,x)\,e^{-i\theta} = h\,(\hat{r},\hat{x})\,e^{-i\hat{\theta}} + \left[\frac{\partial h\,(\hat{r},\hat{x})}{\partial r}(r-\hat{r}) + \frac{\partial h\,(\hat{r},\hat{x})}{\partial x}(x-\hat{x}) - ih\,(\hat{r},\hat{x})\,(\theta-\hat{\theta})\right] e^{-i\hat{\theta}} \tag{3.24}$$

The roll moment induced by the lateral wall can now be computed by integrating Eq. (3.13) with the aid of Eqs. (3.14-3.16, 3.21-3.24).

$$C_{LRM_\ell} = (\tau\, m_L\, a^2 \dot{\phi}^2\, K_1^{\,2})^{-1} \int_{-c}^{c}\int_0^{2\pi} dM_{\hat{x}\ell} = (2\tau c)^{-1} \int_{-c}^{c} R\left\{f_\ell\, \hat{K}^{-1}\right\}_{\substack{r=a\\ x=\hat{x}}} d\hat{x} \tag{3.25}$$

where $$f_\ell = \left[ax\frac{\partial^2 w_s}{\partial r^2} - a^2\frac{\partial^2 w_s}{\partial r\,\partial x} - ia\frac{\partial u_s}{\partial r}\right] Re^{-1} \tag{3.26}$$

$$\hat{K} = K_{10}\, e^{i\phi_{10}} \tag{3.27}$$

Similarly, Eq. (3.17) can be integrated to yield

$$C_{LRM_{e1}} = C_{LRM_{e2}} = (1/2)\, C_{LRM_e} = (2\tau a c)^{-1}\int_0^a R\left\{f_e\, \hat{K}^{-1}\right\}_{\substack{r=\hat{r}\\ x=c}} \hat{r}\, d\hat{r} \tag{3.28}$$

where $$f_e = \left[-r^2\frac{\partial^2 w_s}{\partial x^2} + c\frac{\partial}{\partial x}\left(w_s + iv_s - r\frac{\partial w_s}{\partial r}\right)\right] Re^{-1} \tag{3.29}$$

Finally

$$C_{LRM} = C_{LRM_e} + C_{LRM_\ell} \tag{3.30}$$

In Appendix B it is shown that

$$C_{LRM} = -C_{LSM} + (\tau\varepsilon/2)[1 - (4/3)\ (c/a)^2] \tag{3.31}$$

This equation is valid for linear fluid mechanics and states that for the simple case of constant amplitude motion ($\varepsilon = 0$) the liquid roll moment is the negative of the liquid side moment. If the complete nonlinear fluid equations are used, additional contributions to the quadratic liquid roll moment which are large enough to affect Eq. (3.31) may be present.

IV. DISCUSSION

Reference 2 considers the effect of two types of internal component motion: (a) a mass moving in a circle in a plane normal to the missile's axis; (b) forced coning motion of a spinning component. For these motions the side moment, M_S, and the roll moment, $M_{\tilde{X}}$, were computed and for both cases

$$M_{\tilde{X}} = -K_1\ M_S. \tag{4.1}$$

This is precisely Eq. (3.31) for constant amplitude motion. Equation (4.1) is equivalent to the statement that the liquid moment about the trajectory is zero, i.e.,

$$M_{LX} = 0\ . \tag{4.2}$$

This essentially follows from the linear assumption that the azimuthal velocity about the trajectory varies as exp $(-i\theta)$. A nonlinear theory could well have terms that are independent of θ.

The liquid side moment was computed in Reference 19 for $c/a = 4.291$ and Re from 10^2 to 10^6; the results are given in Figures 2 - 6. Miller[15] observed the roll moment to be independent of roll rate. This means that the liquid roll moment should be proportional to τ. As can be seen from Figures 2 - 6, this is roughly the case for the liquid side moment coefficient. Since Miller's measurements were taken for τ varying from .12 to .25, we will use the liquid side moment coefficient for $\tau = .18$ to compare with Miller's measurements in Figure 1. The agreement is encouraging when we recall that we are applying a linear fluid mechanics calculation to measurements taken at a 20° cone angle and a boundary theory to Reynolds numbers as low as 100.

V. SUMMARY

1. The linear theory for a coning and spinning liquid payload has been extended to the calculation of a quadratic roll moment.

2. The resulting quadratic roll moment coefficient is shown to be exactly the negative of the linear side moment coefficient for constant amplitude coning motion.

3. This relationship between side moment and roll moment has been observed for projectiles with moving solid components and is reasonably well supported by experiment for liquid payloads.

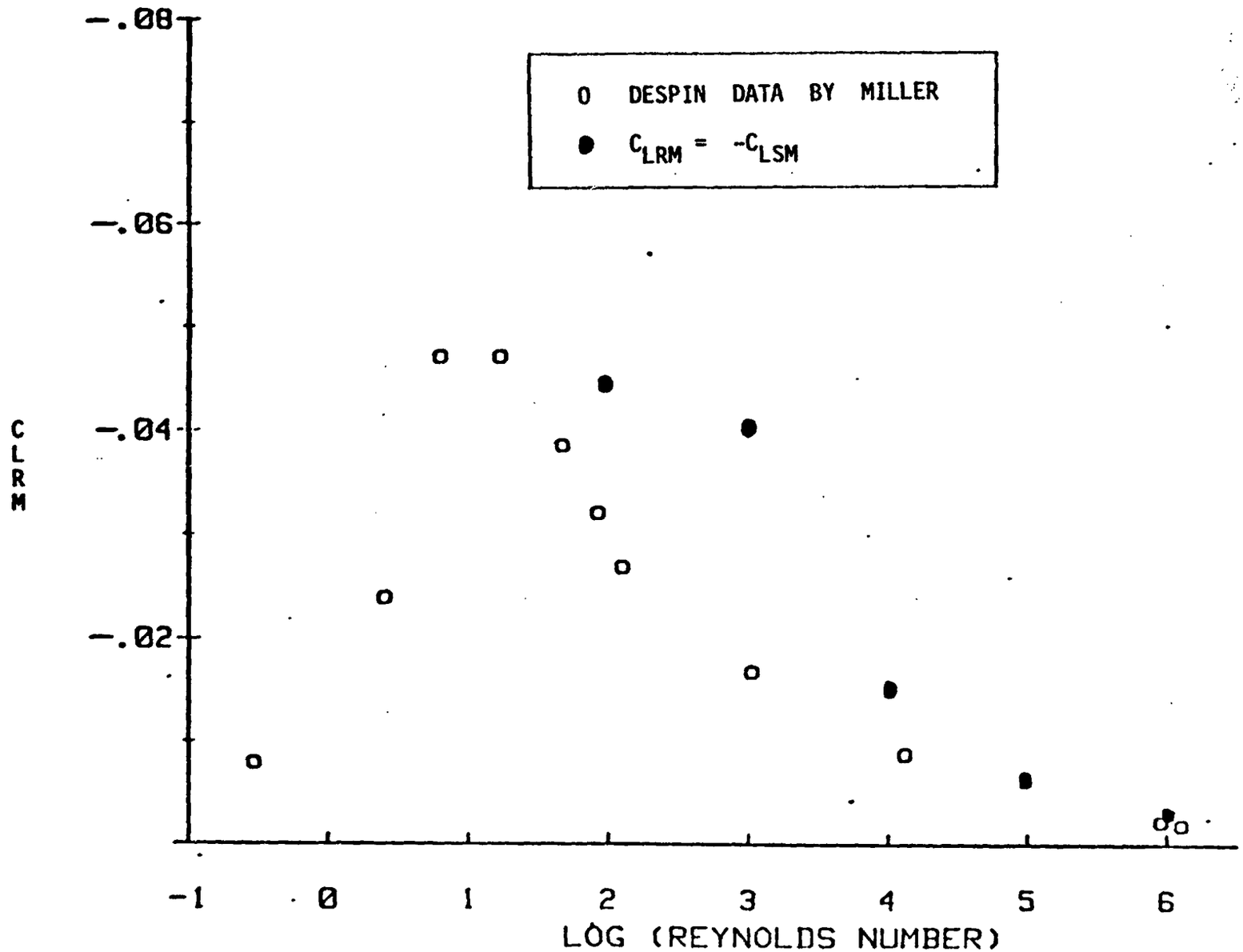

Figure 1. C_{LRM} From Gyroscope Tests (Ref. 15), c/a = 4.291

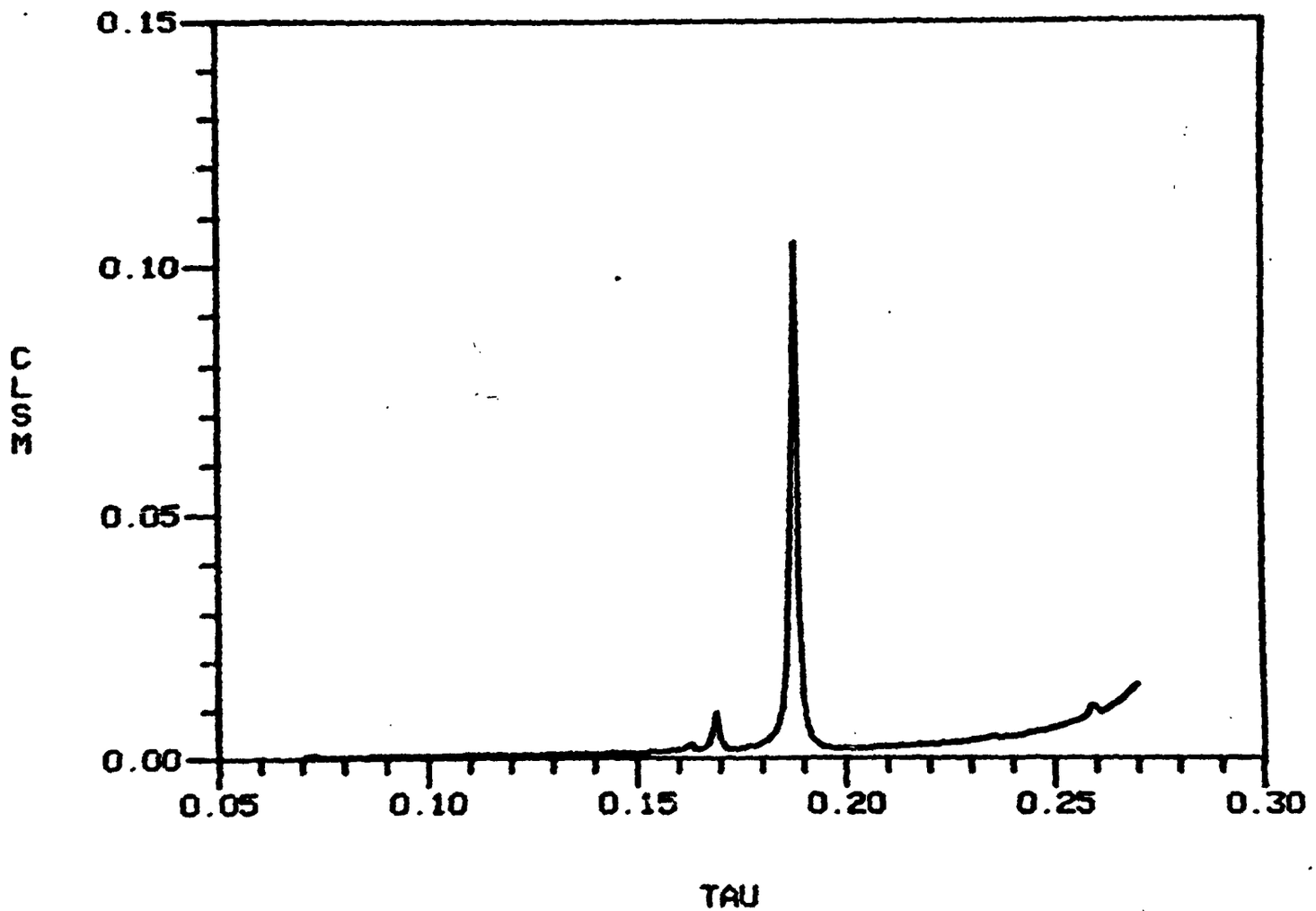

Figure 2. C_{LSM} vs τ for Re = 10^6, ε = 0, and the D'Amico-Miller Parameters: c/a = 4.291, f = 1

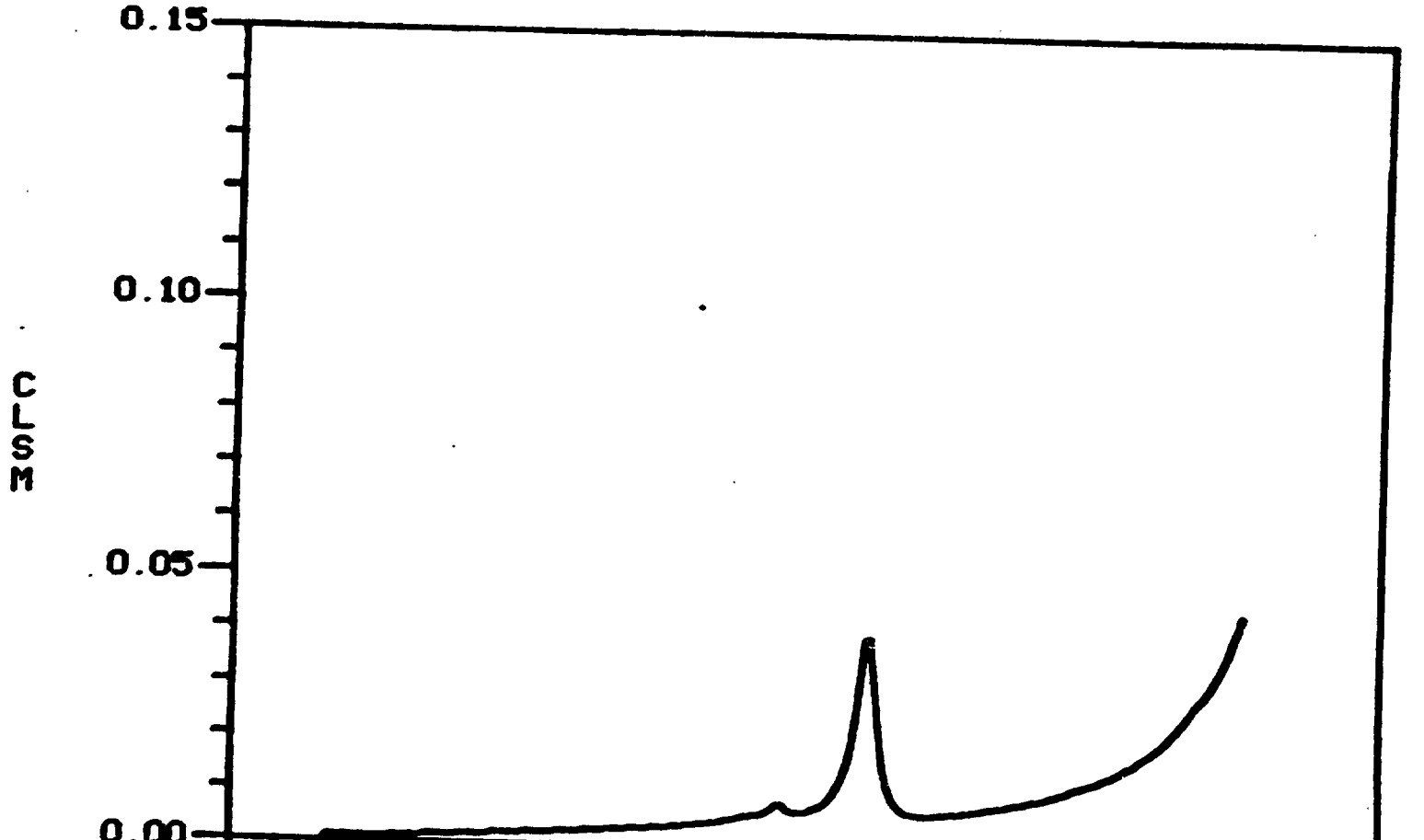

Figure 3. C_{LSM} vs τ for Re = 10^5, ε = 0, and the D'Amico-Miller Parameters: c/a = 4.291, f = 1

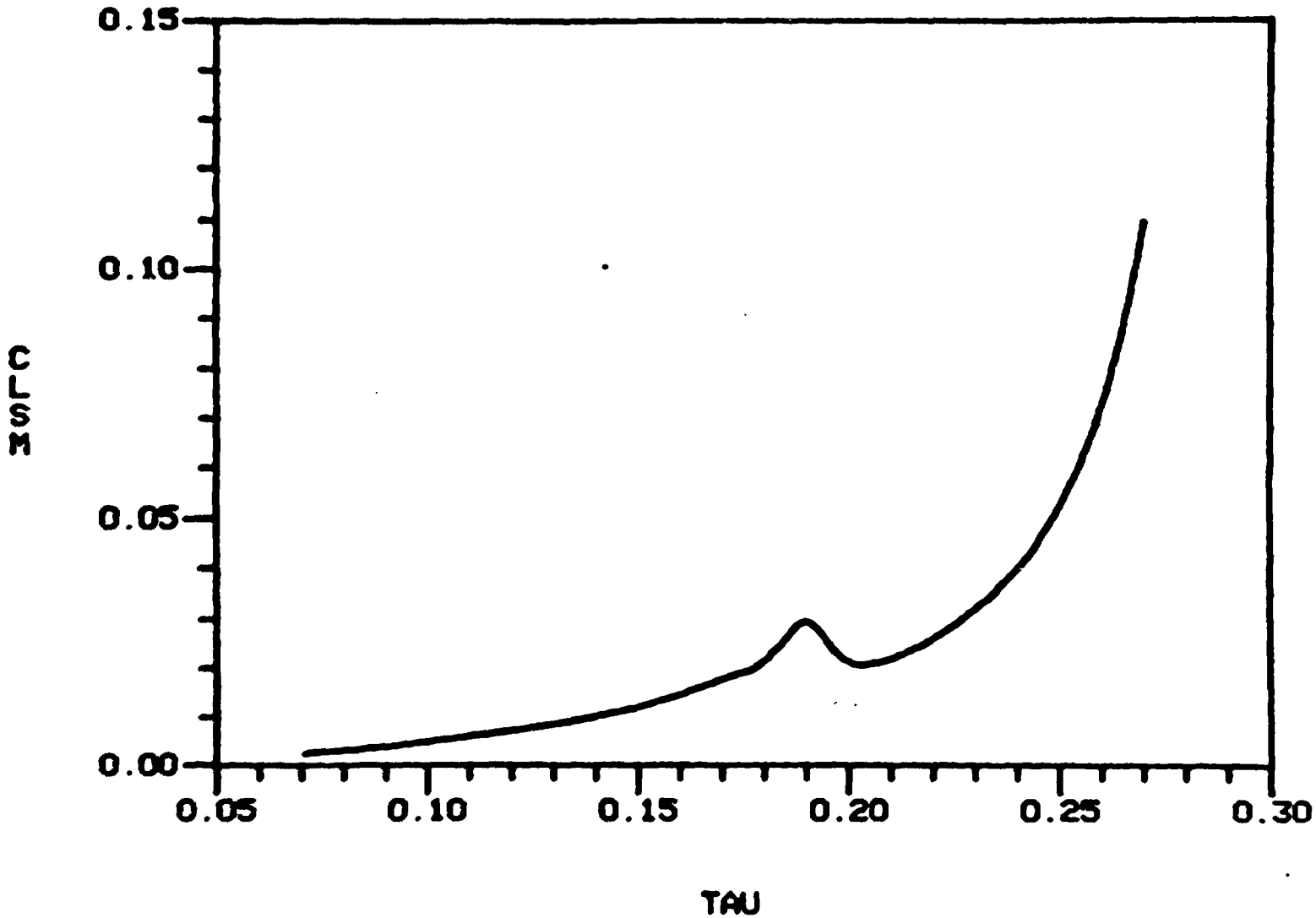

Figure 4. C_{LSM} vs τ for Re = 10^4, ϵ = 0, and the D'Amico-Miller Parameters: c/a = 4.291, f = 1

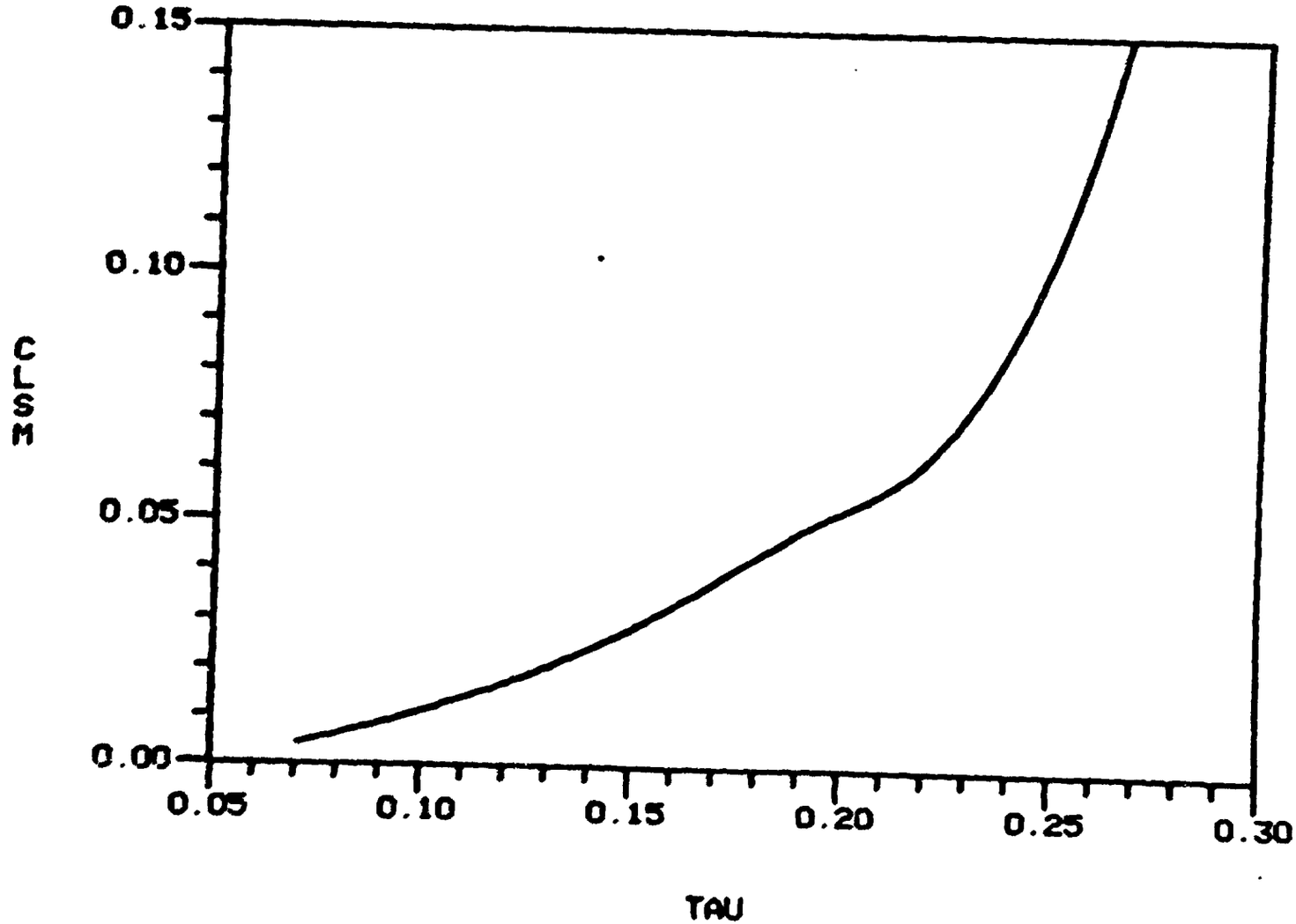

Figure 5. C_{LSM} vs τ for $Re = 10^3$, $\epsilon = 0$, and the D'Amico-Miller Parameters: $c/a = 4.291$, $f = 1$

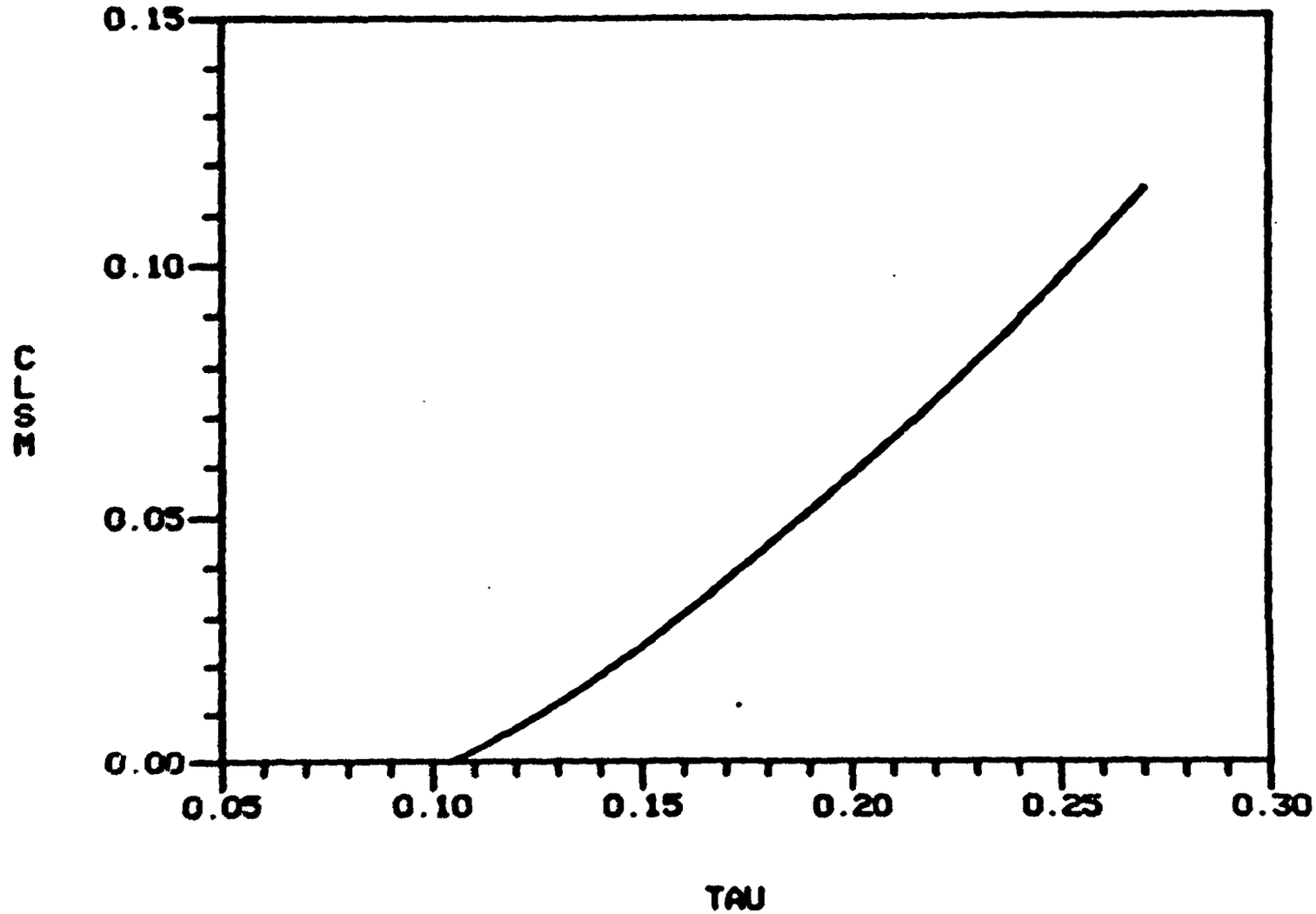

Figure 6. C_{LSM} vs τ for Re = 10^2, ϵ = 0, and the D'Amico-Miller Parameters: c/a = 4.291, f = 1

REFERENCES

1. B.G. Karpov and J.W. Bradley, "A Study of Causes of Short Ranges of the 8" T317 Shell," BRL Report 1049, May 1958 (AD 377548).

2. C.H. Murphy, "Influence of Moving Internal Parts on Angular Motion of Spinning Projectiles," Journal of Guidance and Control, Vol. 1, March-April 1978, pp. 117-122. See also BRL-MR-2731, February 1977 (AD A037338).

3. W.G. Soper, "Projectile Instability Produced by Internal Friction," AIAA Journal, Vol. 16, Jan 1978, pp. 8-11.

4. W.H. Merwagen, "Measurements of the Dynamical Behavior of Projectiles Over Long Flight Paths," Journal of Spacecraft and Rockets, Vol. 8, April 1971, pp. 380-385. See also BRL-MR-2079, November 1970 (AD 717002).

5. W.P. D'Amico, V. Oskay, W.H. Clay, "Flight Tests of the 155mm XM687 Binary Projectile and Associated Design Modification Prior to the Nicolet Winter Test 1974-1975," BRL-MR-2748, May 1977 (AD B019969).

6. W.P. D'Amico, W.H. Clay, and A. Mark, "Yawsonde Data for M687-Type Projectiles with Application to Rapid Spin Decay and Stewartson-Type Spin-Up Instabilities," ARBRL-MR-03027, June 1980 (AD A089646).

7. W.P. D'Amico, W.H. Clay, and A. Mark, "Diagnostic Tests for Wick-Type Payloads and High-Viscosity Liquids," ARBRL-MR-02913, April 1979 (AD A072812).

8. W.P. D'Amico and W.H. Clay, "High Viscosity Liquid Payload Yawsonde Data for Small Launch Yaws," ARBRL-MR-03029, June 1980 (AD A088411).

9. W.P. D'Amico, "Early Flight Experiences with the XM761," BRL-MR-2791, September 1977 (AD B024975L).

10. W.P. D'Amico, "Field Tests of the XM761: First Diagnostic Test," BRL-MR-2792, September 1977 (AD B024976L).

11. W.P. D'Amico, "Field Tests of the XM761: Second Diagnostic Test," ARBRL-MR-02806, January 1978 (AD B025305L).

12. W.P. D'Amico, "Aeroballistic Testing of the XM825 Projectile: Phase I," ARBRL-MR-02911, March 1979 (AD B037680).

13. W.P. D'Amico, "Aeroballistic Testing of the XM825 Projectile: Phase II," ARBRL-MR-03072, January 1981 (AD A098036).

14. W.P. D'Amico, "Aeroballistic Testing of the XM825 Projectile: Phase III, High Muzzle Velocity and High Quadrant Elevation," ARBRL-MR-03196, September 1982 (AD B068511L).

REFEREWCES (Continued)

15. M.C. Miller, "Flight Instabilities of Spinning Projectiles Having Nonrigid Payloads," Journal of Guidance, Control, and Dynamics, Vol. 5, March-April 1982, pp. 151-157.

16. W.P. D'Amico and M.C. Miller, "Flight Instability Produced by a Rapidly Spinning, Highly Viscous Liquid," Journal of Spacecraft and Rockets, Vol. 16, Jan-Feb 1979, pp. 62-64.

17. K. Stewartson, "On the Stability of a Spinning Top Containing Liquid," Journal of Fluid Mechanics, Vol. 5, Part 4, September 1959, pp. 577-592.

18. E.H. Wedemeyer, "Viscous Correction to Stewartson's Stability Criterion," BRL-R-1325, June 1966 (AD 489687).

19. C.H. Murphy, "Angular Motion of a Spinning Projectile With a Viscous Liquid Payload," BRL Memorandum Report ARBRL-MR-03194, August 1982 (AD A118676). See also Journal of Guidance, Control, and Dynamics, Vol. 6, July-August 1983, pp. 280-286.

20. C.W. Kitchens, Jr., N. Gerber, and R. Sedney, "Oscillations of a Liquid in a Rotating Cylinder: Solid Body Rotation," BRL Technical Report ARBRL-TR-02081, June 1978 (AD A057759).

21. N. Gerber, R. Sedney, and J.M. Bartos, "Pressure Moment on a Liquid-Filled Projectile: Solid Body Rotation," BRL Technical Report ARBRL-TR-02422, October 1982 (AD A120567).

22. N. Gerber and R. Sedney, "Moment on a Liquid-Filled Spinning and Nutating Projectile: Solid Body Rotation," BRL Technical Report ARBRL-TR-02470, February 1983 (AD A125332).

23. H.R. Vaughn, "Flight Dynamic Instabilities of Fluid-Filled Projectiles," Sandia Laboratories, Albuquerque, NM, SAND 78-0999, June 1978.

24. C.H. Murphy, "Free Flight Motion of Symmetric Missiles," BRL-R-1216, July 1963 (AD 442757).

25. W.P. D'Amico and R.J. Yalamanchili, "Yawsonde Tests of the 8-Inch XM877 Binary Projectile: Phase I," BRL Memorandum Report in preparation.

26. H. Schlichting, "Boundary Layer Flow," McGraw-Hill Book Company, New York, 1960, p. 54.

APPENDIX A

Errata for Reference 19

APPENDIX A

ERRATA FOR REFERENCE 19

1. Third term of Eq. (5.20) should contain (s - i), not (s - 1).

2. Second line of Eq. (6.4) should read:

$$= i\ (c/2a) \int_{-1}^{1} \hat{x}\ [c_p^*]_{r=a}\ \hat{K}^{-1}\ d\hat{x} + (h/c)^2\ m_{p\ell h} \tag{6.4}$$

3. Eq. (7.1) should read:

$$m_{v\ell} = i\ (2\pi\ \hat{K}\ Re)^{-1}\ e^{-s\phi} \int_{-1}^{1} \int_{0}^{2\pi} e^{i\theta}\ m_{v\ell}^*\ d\theta\ d\hat{x} \tag{7.1}$$

4. Eq. (7.4) should read:

$$m_{ve} = (2a\ \hat{K}\ Re)^{-1} \int_{b}^{a} \left[\hat{x}\ \frac{\partial}{\partial x}\ (w_{sv} - iv_{sv})\right]_{\hat{x}=-1}^{\hat{x}=1} rdr + (h/c)^2\ m_{veh} \tag{7.4}$$

where

$$m_{veh} = (2\ \hat{K}\ Re)^{-1}\ (c/ah) \int_{b}^{a} \left[\frac{\partial}{\partial x}\ (w_{sv} - iv_{sv})\right]_{\hat{x}=-1}^{\hat{x}=1} rdr.$$

5. Third term of Eq. (9.4) should contain (s - i), not (s-1).

APPENDIX B

Relationship Between C_{LRM} and C_{LSM}

APPENDIX B

RELATIONSHIP BETWEEN C_{LRM} AND C_{LSM}

In Reference 19 the pressure parts of the side moment coefficient for the lateral and endwalls are given in Eqs. [6.4 - 6.5].* The viscous shear contributions are given in Eqs. [7.2, 7.4]. These can be combined to yield the complete side moment coefficients for the lateral and endwalls, respectively:

$$C_{LSM_\ell} = (2\tau c)^{-1} \int_{-c}^{c} R \left\{ g_\ell \, \hat{K}^{-1} \right\}_{\substack{r=a \\ x=\tilde{x}}} d\tilde{x} \tag{B-1}$$

$$C_{LSM_e} = (\tau a c)^{-1} \int_{0}^{a} R \left\{ g_e \, \hat{K}^{-1} \right\}_{\substack{r=\tilde{r} \\ x=c}} \tilde{r} \, d\tilde{r} \tag{B-2}$$

where

$$g_\ell = i \, (x/a) \, p_s + \left[x \frac{\partial w_s}{\partial r} + ia \frac{\partial u_s}{\partial r} \right] Re^{-1} \tag{B-3}$$

$$g_e = - i \, (r/a) \, p_s + c \frac{\partial}{\partial x} (w_s - i \, v_s) \, Re^{-1} \tag{B-4}$$

As is shown by Eqs. (3.25 - 3.29), the roll moment coefficients have a very similar form:

$$C_{LRM_\ell} = (2\tau c)^{-1} \int_{-c}^{c} R \left\{ f_\ell \, \hat{K}^{-1} \right\}_{\substack{r=a \\ x=\tilde{x}}} d\tilde{x} \tag{B-5}$$

$$C_{LRM_e} = (\tau a c)^{-1} \int_{0}^{a} R \left\{ f_e \, \hat{K}^{-1} \right\}_{\substack{r=\tilde{r} \\ x=c}} \tilde{r} \, d\tilde{r} \tag{B-6}$$

---

* *Brackets identify equations from Reference 19.*

where

$$f_\ell = \left[ax \frac{\partial^2 w_s}{\partial r^2} - a^2 \frac{\partial^2 w_s}{\partial r \partial x} - ia \frac{\partial u_s}{\partial r}\right] Re^{-1} \tag{B-7}$$

$$f_e = \left[-r^2 \frac{\partial^2 w_s}{\partial x^2} + c\left(r \frac{\partial^2 w_s}{\partial x \partial r} + \frac{\partial w_s}{\partial x} + i \frac{\partial v_s}{\partial x}\right)\right] Re^{-1} \tag{B-8}$$

Since $\frac{\partial^2 w_s(a,x)}{\partial r^2}$ is the dominant term in C_{LRM_ℓ}, it must be computed more carefully than by the usual boundary layer approximation. The linear circumferential momentum equation as given by Eq. [B6] is

$$a^2 Re^{-1} \left[\frac{\partial^2 w_s}{\partial r^2} + \frac{\partial w_s}{r \partial r} + \frac{\partial^2 w_s}{\partial x^2} - \frac{2w_s}{r^2} - \frac{2iv_s}{r^2}\right]$$

$$= (s - i)\, w_s + 2v_s - \frac{iap_s}{r} \tag{B-9}$$

On the boundaries $\hat{r} = a$, $\hat{x} = c$, or $\hat{x} = -c$, v_s and w_s must satisfy the boundary conditions as given by Equations [3.8 - 3.9]:

$$w_s = i\ (s-i)\ (x/a)\ \hat{K} = -iv_s \tag{B-10}$$

Thus, on the boundary surfaces of the liquid container

$$\frac{\partial^2 w_s}{\partial r^2} + \frac{\partial w_s}{r \partial r} + \frac{\partial^2 w_s}{\partial x^2} = a^{-2}\left[-\frac{iap_s}{r} + i\,(s^2 + 1)\ (x/a)\ \hat{K}\right] Re \tag{B-11}$$

On the lateral boundary ($\hat{r} = a$), $\frac{\partial^2 w_s}{\partial x^2}$ is zero and $\frac{\partial^2 w_s}{\partial r^2}$ in Eq. (B-7) can be computed by use of Eq. (B-11). The result can be integrated and simplified by use of Eq. (B-10).

$$C_{LRM_\ell} = -\ C_{LSM_\ell} - (2/3)\ (c/a)^2\ \tau\varepsilon \tag{B-12}$$

Similarly, $\frac{\partial^2 w_s}{\partial r^2}$ and $\frac{\partial w_s}{\partial r}$ are zero on the endwalls ($\tilde{x} = \pm c$) and $\frac{\partial^2 w_s}{\partial x^2}$ in Eq. (B-8) can be eliminated by use of Eq. (B-11)

$$C_{LRM_e} = -C_{LSM_e} + \tau\varepsilon/2 + (\tau\, Re)^{-1} R \left\{ a \frac{\partial w_s}{\partial x} \hat{K}^{-1} \right\}_{\substack{r=a \\ x=c}} \tag{B-13}$$

The derivative of w_s normal to the endwall at the junction of the walls can be computed from Eq. (B-10) and is the same size as the derivatives omitted in the boundary layer approximations of Eqs. (3.18-3.20). Thus, the last term of Eq. (B-13) can be neglected. Eqs. (B-12 - B-13) can then be added to yield the complete liquid roll moment coefficient:

$$C_{LRM} = -C_{LSM} + (\tau\varepsilon/2)\,[1 - (4/3)\,(c/a)^2] \tag{B-14}$$

For constant amplitude coning motion, then, the liquid roll moment is the negative of the liquid side moment.

APPENDIX C

LIQUID ROLL MOMENT FOR PARTIAL FILL

APPENDIX C

LIQUID ROLL MOMENT FOR PARTIAL FILL

If the cylindrical container is only partially filled with liquid, a fully spun-up liquid will fill the space between the outer cylindrical wall and an inner cylindrical free surface with radius b. The ratio of the volume of this inner cylinder to the volume of the complete payload cavity is b^2/a^2. The fill ratio for the payload is, therefore, $1 - b^2/a^2$ and is denoted by f.

In the presence of small amplitude coning motion, this cylindrical free surface is deformed slightly. The equation for this surface in aeroballistic coordinates is

$$\hat{r} = b\,(1 + \eta) \tag{C-1}$$

where

$$\eta = R\left\{\eta_s\,(x)\,e^{s\phi - i\theta}\right\} \tag{C-2}$$

and the perturbation function η_s is linear in $\hat{K}$.

In earth-fixed variables the surface has the form:

$$F\,(x,\ r,\ \theta,\ t) = \hat{x}^2 + b^2\,[1 + \eta]^2 - x^2 - r^2 = 0 \tag{C-3}$$

From Eq. [A12]

$$\hat{x} = x - R\left\{r\,\hat{K}\,e^{s\phi - i\theta}\right\}, \tag{C-4}$$

and η must vary such that the free surface moves with the liquid, i.e.,

$$\frac{DF}{Dt} = V_x\,\frac{\partial F}{\partial x} + V_r\,\frac{\partial F}{\partial r} + \frac{V\theta}{r}\,\frac{\partial F}{\partial \theta} + \frac{\partial F}{\partial t} = 0 \tag{C-5}$$

Equations (C-3) - (C-5) with Equations (3.21 - 3.23) can now be used to obtain an equation for η_s that is linear in $\hat{K}$.

$$b\eta_s\,(x) = x\,\hat{K} + \frac{a v_s(b,x)}{s - 1} \tag{C-6}$$

According to Eq. [B14], at $\hat{x} = \pm c$

$$v_s = \mp (s - i)\ (c/a)\ \hat{K} \tag{C-7}$$

$$\therefore\ \eta_s\ (c) = \eta_s\ (-c) = 0 \tag{C-8}$$

On the free surface, the pressure is constant:

$$\frac{Dp}{Dt} = 0 \tag{C-9}$$

The linear version of this is Eq. [5.8], which was used as the inner boundary condition:

$$(s - i)\ p_s\ (b,x) + (b/a)\ v_s\ (b,x) = 0 \tag{C-10}$$

The side moment coefficient has the same integral relation for C_{LSM_ℓ} as Eq. (B-1), but Eq. (B-2) becomes

$$C_{LSM_e} = (\tau ac)^{-1} \int_b^a R \left\{ g_e\ \hat{K}^{-1} \right\}_{\substack{r=\hat{r} \\ x=c}} \hat{r}\ d\hat{r} \tag{C-11}$$

Similarly, for the liquid roll moment coefficient Eq. (B-5) is unaffected but Eq. (B-6) becomes

$$C_{LRM_e} = (\tau ac)^{-1} \int_b^a R \left\{ f_e\ \hat{K}^{-1} \right\}_{\substack{r=\hat{r} \\ x=c}} \hat{r}\ d\hat{r} \tag{C-12}$$

Eq. (B-13) then becomes

$$\begin{aligned} C_{LRM_e} &= -C_{LSM_e} + (\tau\varepsilon/2)\ [1 - (b/a)^4] \\ &\quad + (\tau a\ Re)^{-1}\ R \left\{ \left[r^2 \frac{\partial w_s(r,c)}{\partial x} \right]_b^a \hat{K}^{-1} \right\} \end{aligned} \tag{C-13}$$

$$\begin{aligned} \therefore\ C_{LRM} &= -C_{LSM} + (\tau\varepsilon/2)\ [1 - (4/3)\ (c/a)^2 - (b/a)^4] \\ &\quad - b^2\ (\tau a\ Re)^{-1}\ R \left\{ \frac{\partial w_s(b,c)}{\partial x}\ \hat{K}^{-1} \right\} \end{aligned} \tag{C-14}$$

LIST OF SYMBOLS

a	radius of a right-circular cylindrical cavity containing liquid
c	half-height of a right-circular cylindrical cavity containing liquid
C_{LIM_j}	fast (j=1) and slow (j=2) mode liquid in-plane moment coefficients; imaginary part of C_{LM_j}.
C_{LM_j}	fast (j=1) and slow (j=2) mode complex liquid moment coefficients defined by Eq. (2.2)
C_{ℓ_p}	aerodynamic roll damping moment coefficient defined by Eq. (2.6)
C_{LRM}	C_{LRM_1} for steady-state coning motion ($K_2 = 0$)
C_{LRM_j}	fast (j=1) and slow (j=2) mode liquid roll moment coefficients defined by Eq. (2.4)
C_{LRM_e}	that part of C_{LRM} induced by the end walls of the cavity
C_{LRM_ℓ}	that part of C_{LRM} induced by the lateral wall of the cavity
C_{LSM}	C_{LSM_1} for steady-state coning motion ($K_2 = 0$)
C_{LSM_j}	fast (j=1) and slow (j=2) mode liquid side moment coefficients; real part of C_{LM_j}
$\vec{e}_{\tilde{x}}, \vec{e}_{\tilde{r}}, \vec{e}_{\tilde{\theta}}$	unit vectors along the aeroballistic cylindrical axes
$e_{\tilde{x}x}, e_{\tilde{x}r}, e_{\tilde{x}\theta}$	components of $\vec{e}_{\tilde{x}}$ in the inertial x, r, θ system
$e_{\tilde{r}x}, e_{\tilde{r}r}, e_{\tilde{r}\theta}$	components of $\vec{e}_{\tilde{r}}$ in the inertial x, r, θ system
$e_{\tilde{\theta}x}, e_{\tilde{\theta}r}, e_{\tilde{\theta}\theta}$	components of $\vec{e}_{\tilde{\theta}}$ in the inertial x, r, θ system
I_x	axial moment of inertia of the projectile
$\hat{K}$	$K_{10} \exp(i\phi_{10})$

K_j	magnitude of the fast (j=1) or slow (j=2) yaw arm
K_{j0}	initial value of K_j
ℓ	reference length
m_L	mass of the liquid in a fully filled cylindrical cavity
$M_{\tilde{L}X}$, $M_{\tilde{L}Y}$, $M_{\tilde{L}Z}$	$\tilde{X}\tilde{Y}\tilde{Z}$ components of the moment exerted by a liquid payload.
r, $\tilde{r}$	radial coordinates in the inertial and aeroballistic systems, respectively
Re	Reynolds number
s	$(\varepsilon + i)\,\tau$
S	reference area
t	time
u_s, v_s, w_s	components of the liquid velocity perturbation in the inertial x, r, θ system
V	magnitude of the missile's velocity
V_x, V_r, V_θ	velocity components in the inertial x, r, θ system
x, $\tilde{x}$	axial coordinates in the inertial and aeroballistic systems, respectively
XYZ	inertial axes; X-axis tangent to the trajectory at time zero.
$\tilde{X}\tilde{Y}\tilde{Z}$	nonrolling aeroballistic axes; $\tilde{X}$-axis fixed along the missile's axis of symmetry
$\tilde{\alpha}$, $\tilde{\beta}$	angles of attack and side-slip in the $\tilde{X}\tilde{Y}\tilde{Z}$ system
γ	$\dot{\psi}/\lvert\dot{\phi}\rvert$
ε_j	nondimensionalized growth rate of K_j
θ, $\tilde{\theta}$	azimuthal coordinates in the inertial and aeroballistic systems, respectively
μ	viscosity

$\tilde{\xi}$	$\tilde{\beta} + i\,\tilde{\alpha}$
ρ	air density
τ	τ_1 for steady-state coning motion ($K_2 = 0$)
τ_j	$\dot{\phi}_j/\dot{\phi}$, the nondimensionalized frequency of the j-th yaw arm (j=1,2)
$\dot{\phi}$	roll rate
ϕ_j	$\phi_{j0} + \tau_j\,\dot{\phi}\,t$
ϕ_{j0}	initial orientation angle of the j-th yaw arm (j=1,2)

DISTRIBUTION LIST

No. of Copies	Organization
12	Administrator Defense Technical Information Center ATTN: DTIC-DDA Cameron Station Alexandria, VA 22314
1	Commander US Army Engineer Waterways Experiment Station ATTN: R. H. Malter P.O. Box 631 Vicksburg, MS 39181
1	Commander US Army Materiel Development and Readiness Command ATTN: DRCDMD-ST 5001 Eisenhower Avenue Alexandria, VA 22333
1	Commander US Army Armament Research and Development Command ATTN: DRDAR-TDC Dover, NJ 07801
3	Commander US Army Armament Research and Development Command ATTN: DRDAR-TSS DRDAR-LC, Dr. J. Frasier Dover, NJ 07801
6	Commander US Army Armament Research and Development Command ATTN: DRDAR-LCA-F Mr. D. Mertz Mr. E. Falkowski Mr. A. Loeb Mr. R. Kline Mr. S. Kahn Mr. S. Wasserman Dover, NJ 07801
1	Director US Army Air Mobility Research and Development Laboratory Ames Research Center Moffett Field, CA 94035
1	Commander US Army Armament Materiel Readiness Command ATTN: DRSAR-LEP-L Rock Island, IL 61299
1	Director US Army ARRADCOM Benet Weapons Laboratory ATTN: DRDAR-LCB-TL Watervliet, NY 12189
1	Commander US Army Aviation Research and Development Command ATTN: DRDAV-E 4300 Goodfellow Blvd St. Louis, MO 63120
1	Director US Army Air Mobility Research and Development Laboratory ATTN: SAVDL-D, W.J. McCroskey Ames Research Center Moffett Field, CA 94035
1	Commander US Army Communications Research and Development Command ATTN: DRSEL-ATDD Fort Monmouth, NJ 07703
1	Commander US Army Electronics Research and Development Command Technical Support Activity ATTN: DELSD-L Fort Monmouth, NJ 07703
1	Commander US Army Missile Command ATTN: DRSMI-R Redstone Arsenal, AL 35898
1	Commander US Army Missile Command ATTN: DRSMI-YDL Redstone Arsenal, AL 35898

DISTRIBUTION LIST

No. of Copies	Organization
1	Commander US Army Missile Command ATTN: DRSMI-RDK, Mr. R. Deep Restone Arsenal, AL 35898
1	Commander US Army Tank Automotive Command ATTN: DRSTA-TSL Warren, MI 48090
1	Commander US Army Jefferson Proving GD ATTN: STEJP-TD-D Madison, IN 47251
2	Commander US Army Research Office ATTN: Dr. R.E. Singleton Dr. Jagdish Chandra P.O. Box 12211 Research Triangle Park NC 27709
1	AGARD-NATO ATTN: R.H. Korkegi APO New York 09777
1	Director US Army TRADOC Systems Analysis Activity ATTN: ATAA-SL White Sands Missile Range NM 88002
2	Commandant US Army Infantry School ATTN: ATSH-CD-CSO-OR Fort Benning, GA 31905
3	Commander Naval Air Systems Command ATTN: AIR-604 Washington, DC 20360
1	AFFDL (J. S. Shang) Wright-Patterson AFB, OH 45433
1	AFWL/SUL Kirtland AFB, NM 87117

No. of Copies	Organization
2	Commander David W. Taylor Naval Ship Research & Development Center ATTN: H.J. Lugt, Code 1802 S. de los Santos Bethesda, MD 20084
1	Commander Naval Surface Weapons Center ATTN: DX-21, Lib Br Dahlgren, VA 22448
4	Commander Naval Surface Weapons Center Applied Aerodynamics Division ATTN: K.R. Enkenhus M. Ciment A.E. Winklemann W.C. Ragsdale Silver Spring, MD 20910
1	AFATL (DLDL, Dr. D.C.Daniel) Eglin AFB, FL 32542
1	AFFDL (W.L. Hankey) Wright-Patterson AFB, OH 45433
5	Director National Aeronautics and Space Administration Ames Research Center ATTN: D.R. Chapman J. Rakich W.C. Rose B. Wick P. Kutler Moffett Field, CA 94035
4	Director National Aeronautics and Space Administration Langley Research Center ATTN: E. Price J. South J.R. Sterrett Tech Library Langley Station Hampton, VA 23365

DISTRIBUTION LIST

No. of Copies	Organization
1	Aerospace Corporation Aero-Engineering Subdivision ATTN: Walter F. Reddall El Segundo, CA 90245
1	Director National Aeronautics and Space Administration Lewis Research Center ATTN: MS 60-3, Tech Lib 21000 Brookpark Road Cleveland, OH 44135
2	Director National Aeronautics and Space Administration Marshall Space Flight Center ATTN: A.R. Felix, Chief S&E-AERO-AE Dr. W.W. Fowlis Huntsville, AL 35812
2	Director Jet Propulsion Laboratory ATTN: L.M. Mach Tech Library 4800 Oak Grove Drive Pasadena, CA 91103
3	Arnold Research Org., Inc. ATTN: J.D. Whitfield R.K. Matthews J.C. Adams Arnold AFB, TN 37389
3	Aerospace Corporation ATTN: H. Mirels R.L. Varwig Aerophysics Lab. P.O. Box 92957 Los Angeles, CA 90009
1	AVCO Systems Division ATTN: B. Reeves 201 Lowell Street Wilmington, MA 01887
3	Boeing Commercial Airplane Company ATTN: R.A. Day, MS 1W-82 P.E. Rubbert, MS 3N-19 J.D. McLean, MS-3N-19 Seattle, WA 98124
3	Calspan Corporation ATTN: A. Ritter G. Homicz W. Rae P.O. Box 400 Buffalo, NY 14225
1	General Dynamics ATTN: Research Lib 2246 P.O. Box 748 Fort Worth, TX 76101
1	General Electric Company, RESD ATTN: W.J. East 3198 Chestnut Street Philadelphia, PA 19101
2	Grumman Aerospace Corporation ATTN: R.E. Melnik L.G. Kaufman Bethpage, NY 11714
2	Lockheed-Georgia Company ATTN: B.H. Little, Jr. G.A. Pounds Dept 72074, Zone 403 86 South Cobb Drive Marietta, GA 30062
1	Lockheed Missiles and Space Company ATTN: Tech Info Center 3251 Hanover Street Palo Alto, CA 94304
3	Martin-Marietta Laboratories ATTN: S.H. Maslen S.C. Traugott H. Obremski 1450 S. Rolling Road Baltimore, MD 21227

DISTRIBUTION LIST

No. of Copies	Organization
2	McDonnell Douglas Astronautics Corporation ATTN: J. Xerikos H. Tang 5301 Bolsa Avenue Huntington Beach, CA 92647
2	McDonnell-Douglas Corporation Douglas Aircraft Company ATTN: T. Cebeci K. Stewartson 3855 Lakewood Boulevard Long Beach, CA 90801
2	Rockwell International Science Center ATTN: Dr. V. Shankar Dr. N. Malmuth 1049 Camino Dos Rios Thousand Oaks, CA 91360
3	Sandia Laboratories ATTN: F.G. Blottner W.L. Oberkampf Tech Lib. Albuquerque, NM 87115
2	United Aircraft Corporation Research Laboratory ATTN: M.J. Werle Library East Hartford, CT 06108
1	Vought Systems Division LTV Aerospace Corporation ATTN: J.M. Cooksey, Chief, Gas Dynamics Lab, 2-53700 P.O. Box 5907 Dallas, TX 75222
1	Arizona State University Department of Mechanical and Energy Systems Engineering ATTN: G.P. Neitzel Tempe, AZ 85281
1	Cornell University Graduate School of Aero Engr ATTN: Library Ithaca, NY 14850
3	California Institute of Technology ATTN: Tech Library H.B. Keller, Math Dept D. Coles, Aero Dept Pasadena, CA 91109
1	Illinois Institute of Tech ATTN: H. M. Nagib 3300 South Federal Chicago, IL 60616
1	The Johns Hopkins University Dept of Mech and Materials Sci. ATTN: S. Corrsin 34th & Charles Street Baltimore, MD 21218
4	Director Johns Hopkins University Applied Physics Laboratory ATTN: Dr. R.D. Whiting Dr. D.A. Hurdif Dr. R.S. Hirsh Mr. E.R. Bohn Johns Hopkins Road Laurel, MD 20707
1	Louisiana State Univeristy Dept. of Physics and Astronomy ATTN: Dr. R.G. Hussey Baton Rouge, LA 70803
3	Massachusetts Institute of Technology ATTN: E. Covert H. Greenspan Tech Lib 77 Massachusetts Avenue Cambridge, MA 02139

DISTRIBUTION LIST

No. of Copies	Organization
2	North Carolina State Univ Mechanical and Aerospace Engineering Department ATTN: F.F. DeJarnette J.C. Williams Raleigh, NC 27607
1	Northwestern University Department of Engineering Science and Applied Mathematics ATTN: Dr. S.H. Davis Evanston, IL 60201
1	Notre Dame University Department of Aero Engr ATTN: T.J. Mueller South Bend, IN 46556
2	Ohio State University Dept of Aeronautical and Astronautical Engineering ATTN: S.L. Petrie O.R. Burggraf Columbus, OH 43210
2	Polytechic Institute of New York ATTN: G. Moretti S.G. Rubin Route 110 Farmingdale, NY 11735
3	Princeton University James Forrestal Research Ctr Gas Dynamics Laboratory ATTN: S.M. Bogdonoff S.I. Cheng Tech Library Princeton, NJ 08540
1	Purdue University Thermal Science & Prop Ctr ATTN: Tech Library W. Lafayette, IN 47907
1	Rensselaer Polytechnic Institute Department of Math Sciences ATTN: R.C. Diprima Troy, NY 12181
1	Rutgers University Department of Mechanical, Industrial, and Aerospace Engineering New Brunswick, NJ 08903
1	San Diego State University Department of Aerospace Engr and Engineering Mechanics College of Engineering ATTN: K.C. Wang San Diego, CA 92182
1	Southern Methodist University Department of Civil and Mechanical Engineering ATTN: R.L. Simpson Dallas, TX 75275
1	Southwest Research Institute Applied Mechanics Reviews 8500 Culebra Road San Antonio, TX 78228
2	Stanford University Dept of Aeronautics/Astronautics ATTN: Dr. J.L. Steger Dr. S. Chakravarthy Stanford, CA 94305
1	Texas A&M University College of Engineering ATTN: R.H. Page College Station, TX 77843
1	University of California - Davis ATTN: H.A. Dwyer Davis, CA 95616

DISTRIBUTION LIST

No. of Copies	Organization
1	University of California - Berkeley Department of Aerospace Engineering ATTN: M. Holt Berkeley, CA 94720
2	University of California - San Diego Department of Aerospace Engineering and Mechanical Engineering Sciences ATTN: P. Libby Tech Library La Jolla, CA 92037
1	University of Cincinnati Department of Aerospace Engineering ATTN: R.T. Davis Cincinnati, OH 45221
1	University of Colorado Department of Astro-Geophysics ATTN: E.R. Benton Boulder, CO 80302
2	University of Maryland ATTN: W. Melnik J.D. Anderson College Park, MD 20740
1	University of Maryland - Baltimore County Department of Mathematics ATTN: Dr. Y.M. Lynn 5401 Wilkens Avenue Baltimore, MD 21228
1	University of Santa Clara Department of Physics ATTN: R. Greeley Santa Clara, CA 95053
2	University of Southern California Department of Aerospace Engineering ATTN: T. Maxworthy P. Weidman Los Angeles, CA 90007
2	University of Michigan Department of Aeronautical Engineering ATTN: W.W. Wilmarth Tech Library East Engineering Building Ann Arbor, MI 48104
2	University of Rochester Department of Mechanical and Aerospace Sciences ATTN: R. Gans A. Clark, Jr. Rochester, NY 14627
1	University of Tennessee Department of Physics ATTN: Prof. W.E. Scott Knoxville, TN 37916
1	University of Texas Department of Aerospace Engineering ATTN: J.C. Westkaemper Austin, TX 78712
1	University of Virginia Department of Aerospace Engineering & Engineering Physics ATTN: I.D. Jacobson Charlottesville, VA 22904
1	University of Virginia Research Laboratories for the Engineering Sciences ATTN: Prof. H. G. Wood P.O. Box 3366 University Station Charlottesville, VA 22903

DISTRIBUTION LIST

No. of Copies	Organization
1	University of Washington Department of Mechanical Engineering ATTN: Tech Library Seattle, WA 98105
1	University of Wyoming ATTN: D.L. Boyer University Station Laramie, WY 82071
3	Virginia Polytechnic Institute and State University Department of Aerospace Engineering ATTN: Tech Library Dr. W. Saric Dr. T. Herbert Blacksburg, VA 24061
1	Woods Hole Oceanographic Institute ATTN: J.A. Whitehead Woods Hole, MA 02543

No. of Copies	Organization
	Aberdeen Proving Ground
	Director, USAMSAA ATTN: DRXSY-D DRXSY-MP, H. Cohen
	Commander, USATECOM ATTN: DRSTE-TO-F
	Director, USACSL, Bldg. E3330, EA ATTN: DRDAR-CLN W. C. Dee
	Director, USACSL, Bldg. E3516, EA ATTN: DRDAR-CLB-PA M. C. Miller DRDAR-CLJ-L DRDAR-CLB-PA DRDAR-CLN